Scientific Research Publishing

Journal of Modern Physics, 2023, 14, 183-197
https://www.scirp.org/journal/jmp
ISSN Online: 2153-120X
ISSN Print: 2153-1196

Hubble Tension versus the Cosmic Evolution of Hubble Parameter in the Unicentric Model of the Observable Universe

Ahmad Hujeirat

IWR, Heidelberg University, Heidelberg, Germany
Email: AHujeirat@iwr.uni-heidelberg.de

How to cite this paper: Hujeirat, A. (2023) Hubble Tension versus the Cosmic Evolution of Hubble Parameter in the Unicentric Model of the Observable Universe. *Journal of Modern Physics*, **14**, 183-197.
https://doi.org/10.4236/jmp.2023.143013

Received: January 1, 2023
Accepted: February 4, 2023
Published: February 7, 2023

Abstract

Recently, a unicentric model of the observable universe (UNIMOUN) was proposed. Accordingly, big bangs are common events in our infinitely large, flat, homogeneous and isotropic parent universe. Their progenitors are clusters of cosmically dead and massive neutron stars that merged after reaching the ultimate lowest quantum energy state, where the matter is in an incompressible superconducting gluon-quark superfluid state and zero-entropy, hence granting the resulting progenitors measurable sizes and immunity to collapsing into black holes. Our big bang happened to occur in our neighbourhood, thereby enduing the universe, the observed homogeneity and isotropy. As the enclosed mass of the progenitor was finite, the dynamically expanding curved spacetimes embedded the fireball started flattening to finally diffuse into the flat spacetime of the parent universe. By means of general relativistic numerical hydrodynamical calculations, we use the $\mathcal{H}$-metric to follow the time-evolution of the spacetime embedding the progenitor during the hadronization and the immediately following epochs. Based thereon, we find that the kinetic energy of newly created normal matter increases with distance in a self-similar manner, imitating thereby outflows of nearly non-interacting particles. On cosmic time scales, this behaviour yields a Hubble parameter, $H(t)$, which decreases slowly with the distance from the big bang event. Given the sensitivity of the data of the Cosmic Microwave Background (CMB) from Planck to the underlying cosmological model, we conclude that UNIMOUN is a viable alternative to ΛCMD-cosmologies.

Keywords

General Relativity: Big Bang, Black Holes, Quasars, Neutron Stars, Quantum Chromodynamics, Condensed Matter, Incompressibility, Superfluidity, Super-Conductivity

1. Introduction

The seminal paper of Edwin Hubble in 1929 about the relation between velocity and distance among extra-galactic objects changed our understanding of the universe entirely and caught Einstein by surprise. He then retracted his static model of the universe and removed the famous cosmological constant Λ. This relation is now known as the Hubble law, and it indicates that distant galaxies recede from each other at much higher rates than their nearby counterparts. Over the last 100 years, the value of the Hubble constant dropped from its initial value of roughly 500 km·s^{-1}·Mpc^{-1} down to approximately 70 km·s^{-1}·Mpc^{-1}, thanks to the continuous improvement of instrumentations in observational astronomy (see [1] [2] [3], and the references therein).

On the other hand, the rapid improvements in instrumentations in observational astronomy have recently highlighted discrepancies among key cosmological parameters. While the Planck data of the CMB radiation reveals that the Hubble constant is H_0 = 67.27 ± 0.66 km/s/Mps, the Type Ia supernova measurements yield H_0 = 73.2 ± 1.3 km/s/Mps [4] [5]. The precisions of these predictions are, unfortunately, not model-independent, but certain a priori assumptions related to the topology of spacetime and to ΛCDM-cosmologies[1] are inherently included. These in turn rely directly or indirectly on components that are poorly understood, such as inflation, dark matter, and dark energy [6] [7] [8] [9], for which there are no remedies in sight. Continuing to rely on these models may delay the appearance of new consistent models of the universe.

Recently UNIMOUN has been presented. It is a general relativistic (-GR) model and relies neither on inflation nor on dark matter and/or dark energy. It revives Einstein's objection to the existence of black holes. Still, it incorporates components from quantum field theory (QFT) and chromodynamics, such as incompressibility and superfluidity of gluon-quark matter [10] [11] [12]. Also, it hypothesizes a connection between general relativity and QFT that spacetimes embedding SuSu-cores must be conformally flat. Here SuSu-matter is the state of supranuclear dense matter with zero entropy, where the matter is said to be in incompressible superconducting gluon-quark superfluid phase [13].

The motivations underlying this hypothesis may be summarized as follows:

- The well-observed glitch phenomena in pulsars [14] [15] and the merger of the neutron stars in GW170817 [16] suggest that massive pulsars may be born with embryonic cores that are made of incompressible superconducting gluon-quark superfluids with zero entropy [12], (*i.e.* SuSu-matter). The density here is equal to the maximum possible density permitted in our universe [10], ρ_{max}^{uni}, which is predicted to be $[3\rho_0 \le \rho_{max}^{uni} \le 5\rho_0]$. These embryonic cores serve as seeds in a universal life cycle that leads to the formation of the next generations of big bangs (see **Figure 1**).
- The GR field equations are incapable of treating incompressible SuSu-matter self-consistently [17]. In fact, the causality condition requires the pressure in

[1]CDM stands for Cold Dark Matter.

SuSu-matter to be upper-limited by the constant energy density, thereby blocking the regime of ultrabaric state of matter [18]. However, as long as the embedding spacetime is not flat, this causality condition under these circumstances will be violated. In this case, each side of the GR field equations must vanish at every event of the spacetime embedding the core, *i.e.* $G_{\mu\nu} = T_{\mu\nu} = 0$. A reliable astrophysical situation requires a new type of matter, such as the incompressible SuSu-matter, which sets to evolve in space and time as dictated by an intrinsically time-dependent metric.

Indeed, the matter inside the cores of glitching pulsars, e.g. the Crab and Villa pulsars, are expected to obey these conditions nicely [19].

- Geometrical locations in incompressible SuSu-cores are ill-defined [20]; the interiors of these cores are completely uniform, homogeneous and isotropic. Unlike normal stars, where the gradient of any physical quantity has to fulfil the regularity condition at the centre serve, in SuSu-cores however, these conditions are fulfilled at every event, save the confining surface, where the coupling information between all its constituents are mirrored and encoded in a holographic manner as proposed by the holographic principle [21].
- Both the homogeneity and isotropy of both the observable universe and the interior of SuSu-cores imply that the decaying front must have started at the surface and not in the interior of SuSu-cores.This also may explain why the progenitor of our BB escaped the collapse into a hypermassive black hole (BH).

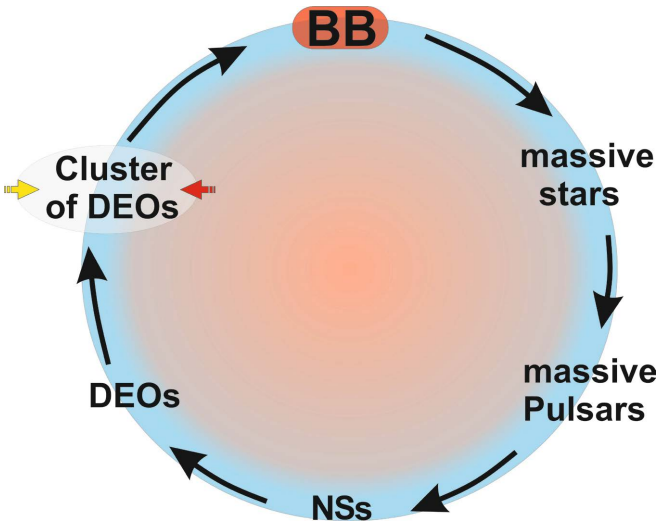

Figure 1. A schematic description of the life cycle of an arbitrary unicentric universe: It starts with a big bang explosion (**BB**) through which the first generation of massive stars are formed and subsequently collapse to generate the first generation of massive pulsars, that evolve toward neutron stars (**NSs**). As these degenerate stars cool down on cosmic time scales, the masses and dimensions of their SuSu-cores grow to finally turn into invisible dark energy objects (**DEOs**). These objects start conglomerating on relatively long time scales to form tight clusters of DEOs, some of which may originate from the ambient parent universe. Once merged, they create the progenitors for the next generation of big bangs.

When applying these arguments to the evolution of our universe, the following universal life cycle emerges: It starts with a big bang explosion triggered by the hadronization process of the progenitor, which is expected to last for roughly one hour or less, then the jettisoned normal matter in the ambient space cools down, contracts and subsequently forms the first generation of massive stars. These stars are predicated to form from the gravitationally bound normal matter inside the local universe after the hadronization process has been completed, which implies that the epoch of formation of the first generation of stars may have been completed much earlier than in the models based on ΛCDM-cosmologies. However, once they are formed, these objects are short-living and eventually doomed to collapse and form the first generation of massive pulsars that subsequently evolve into massive NSs. These, in turn, continue to liberate their rest energies whilst their SuSu-cores grow in mass and dimension to finally metamorphose into invisible DEOs [Dark energy in DEOs and in cosmology are different by construction. In the former case, the pressure is not a local thermodynamical quantity (see [10], and the references therein)]. In the following epoch, DEOs start conglomerating toward forming tight clusters that subsequently merge and form the progenitors for the next generations of big bangs. In this picture, the DEOs that formed the progenitor may not necessarily originate from the same perturbed sub-universe containing the BB but may originate from multiple sub-universes as depicted in **Figure 1**. The origin of our observable homogenous and isotropic universe is a big bang that happened in our neighbourhood, hence the model's name. The main properties of UNIMOUN may be summarised as follows:

- Our observable universe is a submanifold of our infinitely large and flat parent universe.
- Big bangs are frequent events through which limited topological deformations of the embedding spacetime are triggered but ultimately diffuse out into the infinitely large and flat parent universe.
- The occurrences of BBs are self-sustained processes (see **Figure 1**), that evolve without invoking exotic and/or external forces/phenomena, such as inflation [9], dark matter [22] and dark energy [7].
- The BB-progenitors are made of SuSu-matter, which enables the progenitors to be of finite, measurable sizes and prevent their collapse into hypermassive black holes.
- Our BB must have occurred in our neighbourhood, and therefore may explain the observed homogeneity of the universe. However, the isotropic character has been retained after billions of years, when the initially curved spacetime finally diffused into the infinitely large and flat parent universe.
- The observed receding velocities of high redshift galaxies are consequences of extensive matter and momentum transfer from the fireball-matter into the then old and inactive ones that populated the ambient spacetime.

2. The Analytical and Numerical Approach

Our analytical and numerical approaches are based on solving the GR time-

dependent field equations using the [4 × 4] diagonal $\mathcal{H}$-metric [23]:

$$\mathrm{ds}_H^2 = \sum g_{\mu\nu}\mathrm{d}x^\mu \mathrm{d}x^\nu, \tag{1}$$

where the non-zero diagonal elements of the metric g, read:

$$\begin{aligned} g_{00} &= \mathrm{e}^{2\mathcal{V}(r,t)} = 1-\chi(r,t) \\ g_{11} &= \mathrm{e}^{2\lambda(r,t)} = -\frac{1}{1-\chi(r,t)} \\ g_{22} &= -r^2,\ g_{33} = -r^2\sin^2\theta, \end{aligned} \tag{2}$$

where $\mathcal{V},\lambda$ are functions of the distance r and time with respect to $\mathcal{H}_0$, respectively. Here both indices μ and ν run from 0 to 3, and $\mathcal{X}(r,t)$ is the curvature function defined as:

$$\mathcal{X}(r,t) = \alpha_{bb}\frac{m_n(r,t)}{r}. \tag{3}$$

$m_n(r,t)$ here corresponds to the enclosed mass of normal matter only, and α_{bb} is the so-called compactness parameter.

In this model, only normal matter is set to interact with the embedding spacetime and affect its topology. As the progenitor is made of incompressible SuSu-matter with vanishing entropy, $m_n(r,t\le 0)=0$ is set to vanish. Hence prior to hadronization, the topology of the spacetime embedded the progenitor was indistinguishable from that of the parent spacetime. At $t=0$ the hadronization front formed at the surface of the progenitor and started propagating inwards, converting SuSu-matter into normal matter. During this hadronization phase, $m_n(r,t)$ set to increase continuously, thereby enhancing the curvature of the embedding spacetime.

The topological changes of the spacetime are calculated using the following equation (see [20] [23], for the derivation):

$$\begin{aligned} &\frac{1}{2r}\left[\frac{\partial}{\partial t}\left(\mathrm{e}^{-2\mathcal{V}}\right)+\frac{\mathrm{e}^{-2\lambda}}{\mathrm{e}^{-2\mathcal{V}}}\frac{\partial}{\partial r}\left(\mathrm{e}^{-2\mathcal{V}}\right)+\frac{\partial}{\partial r}\mathrm{e}^{-2\lambda}\right] \\ &= -\frac{1}{2}\kappa(\mathcal{E}+p)\left[\Gamma^2\left(g_{00}-V^2g_{11}\right)\right] \\ &= -\frac{1}{2}\kappa(\mathcal{E}+p)\bar{\bar{\Gamma}}, \end{aligned} \tag{4}$$

where Γ is the Lorentz factor, whereas $\bar{\bar{\Gamma}}$ corresponds to the modified Lorentz factor:

$$\bar{\bar{\Gamma}}^2 = \begin{cases} \dfrac{g_{00}+V^2g_{11}}{g_{00}-V^2g_{11}} & : \text{Generalform} \\ 1 & : \text{Hydrostatic cores embedded in curved spacetimes} \\ \dfrac{1+\beta^2}{1-\beta^2} & : \text{Flatspacetime.} \end{cases} \tag{5}$$

In fact, $\bar{\bar{\Gamma}}$ was identified in [23] to be more inductive to the state of matter embedded in dynamically varying spacetimes than the classical Lorentz factor

Γ.

We term the function $\mathcal{V}(r,t)$ as the "gravitational potential" and r is the distance from the preferred observer $\mathcal{H}_0$ located at the center of the progenitor, *i.e.* at $r=0$.

Equation (4) is solved together with the time-dependent equations of mass and momentum transfer, which read:

$$\begin{aligned}&\left(\frac{1}{\sqrt{-g}}\frac{\partial}{\partial t}\left(\sqrt{-g}\mathcal{D}\right)+\frac{1}{\sqrt{-g}}\frac{\partial}{\partial r}\sqrt{-g}\left(\mathcal{D}V\right)\right)=0\\&\frac{1}{\sqrt{-g}}\frac{\partial}{\partial t}\left(\sqrt{-g}\mathcal{M}^r\right)+\frac{1}{\sqrt{-g}}\frac{\partial}{\partial r}\left(\sqrt{-g}\mathcal{M}^rV\right)=-\frac{\partial P}{\partial r}+\frac{\mathcal{M}^t}{2}\left(g_{tt,r}+V^2g_{rr,r}\right).\end{aligned}\tag{6}$$

$V,\mathcal{D}$ here are the transport velocity and relativistic density, *i.e.* the normal rest density times the Lorentz factor. $\sqrt{-g}\left(=r^2R^3\sin(\theta)/\sqrt{GW}\right)$ is the determinant of the $\mathcal{H}$-metric. $\mathcal{M}^\sigma\left(\doteq\mathcal{D}hu^\sigma\right)$ and u^σ stand for the four-momenta and four-velocities (in $\sigma=\{t,r,\theta,\varphi\}$ coordinates), respectively, whereas h stands for the enthalpy. To close the set of equations, an adiabatic equation of state (EOS) is used.

The above set of equations is solved implicity in combination with the finite-volume strategy and within the framework of the operator-splitting approach strategy (see [24] [25] for further details).

The hydrodynamical calculations are run using the following initial conditions:

- The initial mass of the progenitor is $M_p=10^{24}M_\odot$, which is solely made of incompressible SuSu-matter. $M_\odot$ here is solar mass.
- The spacetime inside and outside the progenitor is initially flat. This is a consequence of the underlying hypothesis that SuSu-matter with zero-entropy is neither capable of interacting nor affecting the topology of the embedding spacetime (This addresses the possibilities that there might be a hidden connection between gravity and entropy [26]).
- At $t=0$, the membrane confining the incompressible SuSu-matter in the entire progenitor is removed, and as a consequence, a hadronization front forms at the progenitor's surface and start propagating inwards with speed V_f, thereby converting SuSu-matter into the normal matter at a rate (non-dimensional):

$$\dot{M}^{nor}=\begin{cases}1+t^2-2t & :\ 0\le t\le\tau_{dyn}\\0 & :\ t>\tau_{dyn},\end{cases}\tag{7}$$

thereby increasing the mass of normal matter at the rate:

$$M^{nor}=\begin{cases}3t-3t^2+t^3 & :\ 0\le t\le\tau_{dyn}\\1 & :\ t>\tau_{dyn}\end{cases}\tag{8}$$

where τ_{dyn} is the dynamical time scale, which is equal to the radius of the progenitor r_p divided by V_f. In the present calculations, we set $V_f=0.9999$ in the unit of c. As the density of SuSu-matter is $\rho=\rho_{uni}^{max}=3\rho_0$, we obtain a pro-

genitor's radius $r_p = 8.38\times10^{13}$ cm and $\tau_{dyn} = 2.79\times10^{3}$ s. We use $M_p = (4\pi/3)\rho_{cr} r_0^3$ and $\dot{M}^{nor}$ in $\left(4\pi r_0^2\right)\times\left(\rho_{cr} V_f\right)$ as reference quantities for non-dimensionalizing the equations.

Based thereon, we show in Figure 2 the time-evolution of the radial velocity V, the modified Lorentz factor $\bar{u}^t\left(\doteq\bar{\bar{\Gamma}}\right)$ and the gravitational redshift Z_{grav} during the hadronization and the immediately following epochs. The achieved time here is $11\tau_{dyn}$, which is equivalent to the first 7.5 hours of the big bang explosion.

The results obtained here reconfirm the following arguments:

- Both the radial velocity and the kinetic energy per mass, increase with the distance self-consistently, *i.e.* $\mathrm{d}V/\mathrm{d}r > 0$, and don't violate the causality condition.

In the very outer shells of the progenitor, the newly created normal matter is jettisoned into the surrounding flat spacetime with ultra-relativistic velocities, almost unaffected by the curved topology of the embedding spacetime, as the total available mass of normal matter, $m_n(r,t)$ is still small, relatively.

During hadronization, the gravitational well in the central regions of the fireball becomes increasingly deeper, enforcing thereby the newly created normal matter here to lose a considerable part of its kinetic energy to overcome the potential well. This may be considered as enforced balance between outward advection of momentum and deceleration through curvature:

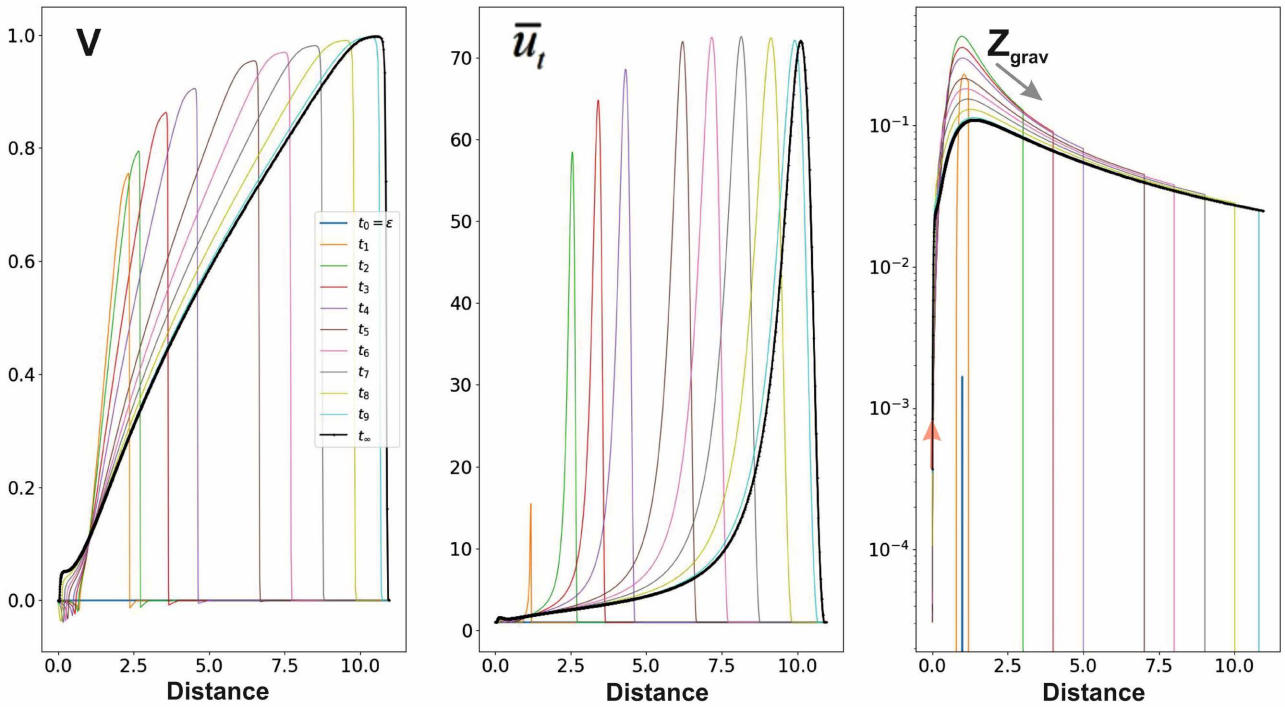

Figure 2. Different snapshots of the radial distributions of the velocity V, the modified Lorentz factor $\bar{\mathbf{u}}^t$ and the gravitational redshift Z_{grav}, during the hadronization and the immediately following epochs. The time-sequence of the snapshots are marked with different colours, starting with blue and ending with black. The tendency of flattening of the spacetime is emphasized by two arrows in the third panel of Z_{grav}.

$$\frac{1}{\sqrt{-g}}\frac{\partial}{\partial r}\left(\sqrt{-g}\mathcal{M}^r V\right)\approx\frac{\mathcal{M}^t}{2}\left(g_{tt,r}+V^2 g_{rr,r}\right). \tag{9}$$

when this equation is integrated over volume and simplified, we obtain the usual balance of potential energy and kinetic energy prescribed by Newtonian mechanics:

$$V^2(r)-V_f^2\approx g_{tt,r}\left(r-r_f\right). \tag{10}$$

In the early stages of the hadronization epoch, $g(t)_{tt,r}$ in the outer shells is negligibly small, and therefore the propagational velocity, V and the jettisoniing/detonation velocity, V_f become almost identical. Once the hadronization process has been completed, then the deep gravitational well must have reached its maximum, and therefore particles in the very central region must lose considerable fractions of their kinetic energies to climb up the potential well. This is a consequence of the spatially and temporarily varying topology of the spacetime embedding the expanding fireball, which differs fundamentally from the stationary spacetimes, such as the Schwarzschild one, where $g_{tt,r}$ attains its maximum at the surface of the object.

Both plots of V and $\bar{u}^t$ show that the bulk of the kinetic energy is transported outwards, where the velocity converges to V_f, thereby giving rise to a constant outflow rate in which $\rho\sim 1/r^2$. This trend has been made possible as the gravitational redshift tends to decrease with time, as depicted with arrows in the third panel of **Figure 2**. As the spacetime embedding the fireball expands, its curvature must flatten with time as prescribed by the minimum energy theorem (see [10], and the references therein).

- In **Figure 3** we show different snapshots of V and $\bar{u}^t$ in the innermost region. Here the low and inward-oriented motion implies that the newly created normal matter is trapped in the fireball's potential well, therefore slowing its motion and delaying its escape into the ambient flat spacetime. However, the potential well is not sufficiently deep to trigger a collapse of the matter in the central regions into a BH. On cosmic scales, the matter here is expected to cool down and form the galaxies of our local universe, whose redshifts are relatively small.

The Cosmic Evolution and the Hubble Parameter

Prior to the big bang explosion, the progenitor was levitating at the background of our infinitely large and flat parent universe, which populated all types of galaxies and objects. UNIMOUN predicts the spacetime surrounding the progenitor of our big bang to have been populated, but with at least 13.8 Gyr old and inactive galaxies. When the outward-propagating normal matter of the expanding fireball hit the surrounding galaxies with the ultra-relativistic speeds, mass with enormous momentum was transferred to these galaxies, turning them active and setting them into outward-oriented motions, whose increase rates depend on different parameters, and mainly on their cross-sections, masses and distances from the BB-event [20].

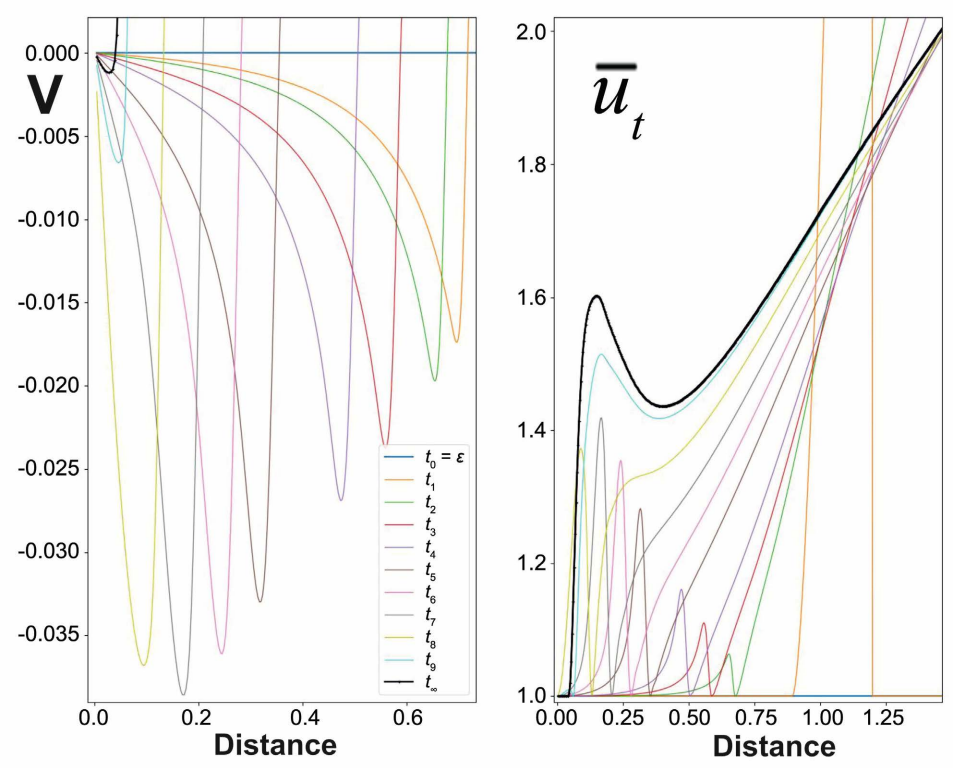

Figure 3. The hydrodynamics of the newly created normal matter in the central region during the hadronization phase and thereafter is shown through a time-sequence of snapshots of the radial velocity, V and the modified Lorentz factor $\overline{u}^t$. The small negative radial velocity, though relatively small, which is a consequence of the relatively high compactness of the progenitor, would considerably slow the receding velocities of the galaxies formed in the vicinity of the big bang. In the right panel, the continuous flattening of the spacetime embedding the fireball is sketched in accord with the minimum energy theorem.

As the observable effect of momentum transfer may need much longer time than the dynamical time scale of the progenitor, we need to integrate Equations (6) over the volume of the smallest spherical sector enclosing a prototype of an old inactive galaxy. In this case, the integration of the continuity equation yields:

$$\frac{\delta\mathcal{M}}{\delta t}+\left(\dot{\mathcal{M}}_o-\dot{\mathcal{M}}_{in}\right)=0, \tag{11}$$

where $\delta\mathcal{M}, \dot{\mathcal{M}}_{in}\left(=A^G_{cone}\mathcal{D}V\right)$ and $\dot{\mathcal{M}}_o$ stand for the total mass absorbed by the galaxy and mass inflow in and outflow from the galaxy, respectively. A^G_{cone} is the cross-section of the spherical sector of the cone enclosing the concerned galaxy located at r_G. For $r_G \gg r_p$, the spacetime surrounding the galaxy is set to be initially flat.

For simplicity, we consider the mass ejection rate out of the galaxy to be $\dot{\mathcal{M}}_o=\alpha\dot{\mathcal{M}}_{in}$, where $\alpha<1$. Moreover, we assume the collision between the normal matter of the expanding fireball with the motionless galaxy to be inelastic, *i.e.*,

$$\delta\mathcal{M}\beta_{in}+M_G\beta_G^{\nearrow 0}=\left(\delta\mathcal{M}+M_G\right)\beta_f, \tag{12}$$

where $\beta_{in}, \beta_G, \beta_f$ are the inflow velocity of normal matter through the left boundary of the galaxy, the velocity of the galaxy prior collision, which is set to vanish, and the final combined velocity of the galaxy together with the captured matter, respectively. $\mathcal{M}_G$ stands for the mass of the galaxy. In this case, the final velocity of the combined object reads:

$$\frac{\beta_f}{\beta_{in}} = \frac{\delta\mathcal{M}}{M_G + \delta\mathcal{M}} = \frac{(1-\alpha)\dfrac{\beta}{\sqrt{1-\beta^2}}t}{M_G + (1-\alpha)\dfrac{\beta}{\sqrt{1-\beta^2}}t}, \tag{13}$$

where we inserted $\delta\mathcal{M}$ from the integrated continuity equation (Equation (11)).

For $M_G > 0$, the causality condition is satisfied self-consistently.

In Figure 4 the final velocity of the bombarded galaxy is plotted versus time (in τ_{dyn} units) for different injection/ejection rates and masses. Here the following trends may be identified:

- Independent of M_G and $\dot{\mathcal{F}}$, the acceleration rate of all galaxies is almost identical.
- Massive or distant galaxies require, as expected, much longer times to accelerate their outward motions compared to low masses or close ones.

Based thereon, the fireball may have affected the observed galaxies at least in three different ways (see Figure 5):

- Type G_A galaxies may have formed after the BB and populated the local universe. Their relative motions may not be well-defined, though they must have slow-receding velocity components. These receding velocity components are direct consequences of the expanding spacetime embedding the expanding fireball enclosing a finite mass of normal matter. Following the minimum energy theorem, the spacetime must flatten as depicted by the arrows in Panel 3 of Figure 2.
- Old and inactive galaxies, G_B, that populated the spacetime surrounding the BB then at intermediate distances from the BB event. The cross-sections and distances of these galaxies should have laid in a certain regime of parameters, which allows them to gain sufficient mass and momentum and still accelerate their outward-oriented motions without deforming their internal structures completely. Meanwhile the gained mass-momentum enabled them to reach ultra-high relativistic velocities, and currently, they populate the very outer regions of the observable universe.
- Relatively remote, old and inactive galaxies, G_G, that populated the parent universe, should have been hit by the expanding fireball of the BB. Due to their low effective cross sections, the overall gained mass and momentum were relatively low. Still, they were sufficient to turn them on and accelerate their outward-oriented motions up to intermediate values.

For the given dependence of β_f on time, the corresponding Hubble parameter reads:

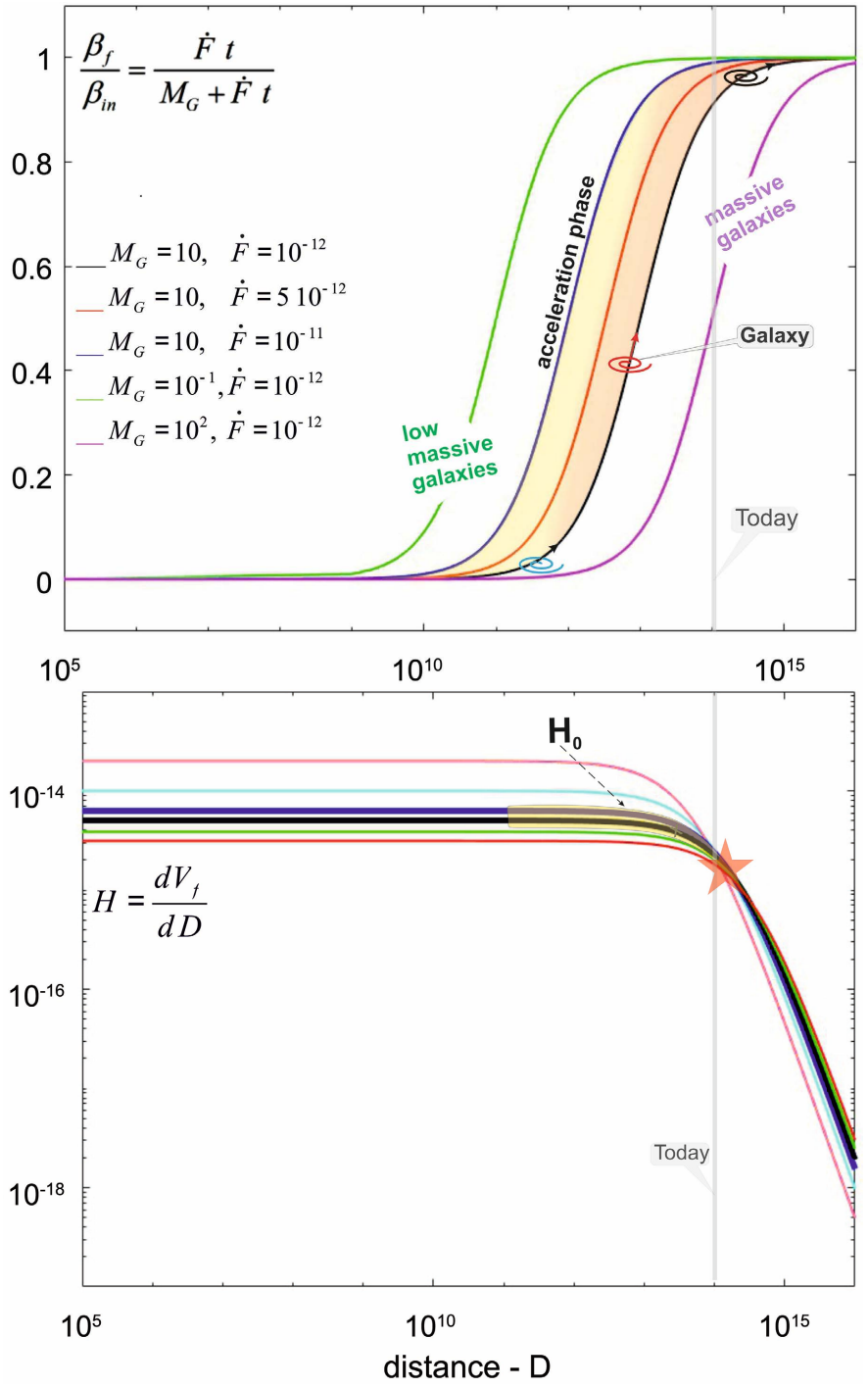

Figure 4. The time-development of the receding velocity of galaxies for different galaxy masses and incident fluxes $\dot{F}$ (top). The blue, red and black lines correspond to galaxies having the same mass $M_G = 10$ and incident fluxes $\dot{F} = 10^{-11}, 5\times10^{-12}, 10^{-12}$, respectively. The green and cyan lines correspond to low and massive galaxies, respectively. In the lower panel, the Hubble parameter, $H = \mathrm{d}V/\mathrm{d}D$ is shown for different galaxy masses and incident fluxes. In all cases, the H decreases slowly with the cosmic time, *i.e.* with distance, though at different rates. Galaxies with high effective masses display relatively lower Hubble constants, but in roughly 21 Gyr from now, the different values converge to a single value, beyond which H evolves reversibly.

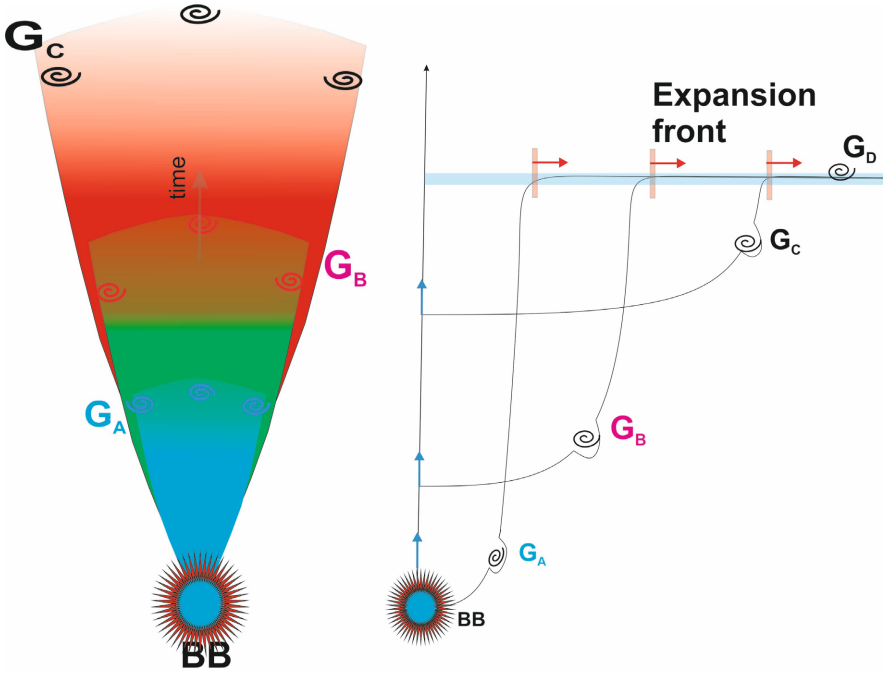

Figure 5. A schematic description of the three types of galaxies that may affect the time-evolution of the Hubble "constant." G_A are galaxies that were formed from the newly created normal matter in the central region of the fireball. The matter here must have been anchored deeply in the gravitational potential-well of the fireball and therefore have relatively low kinetic energy. G_B are the old inactive galaxies that have been hit by the fireball, absorbed an enormous amount of mass and momentum and were forced to accelerate their radially oriented motion relatively fast and later became to high redshift galaxies. G_C are relatively distant old and inactive galaxies that have been hit by the fireball and subsequently turned into an active mode whilst accelerating their outward velocities. G_D are galaxies that populate the parent universe and are beyond the particle horizon.

$$H = \frac{\mathrm{d}V}{\mathrm{d}D} = \frac{\mathrm{d}\beta_f}{\mathrm{d}t}. \tag{14}$$

In Figure 4, $H(t)$ is plotted for different injection rates between $[10^{-12} \le F \le 10^{-11}]$. Here $\mathrm{d}V/\mathrm{d}D$ is not really a constant but rather a slowly varying function of time. In the early universe, $H(t)$ had higher values than in the late universe. This suggests that when the normal matter of the expanding fireball hit the first G_B-type galaxies, it set them into an acceleration mode relatively early, and they currently should have reached higher redshifts than their distant counterparts. In fact, their close distance to the BB event makes their effective cross-sections relatively larger, and therefore the possibility of absorbing normal matter and momentum would be much higher. For causality reasons, this trend must change: extremely high redshift galaxies cannot continue increasing their velocities with distance indefinitely but eventually converge to a constant velocity, namely to the incident velocity V_f. On the other hand, those initially distant galaxies would continue increasing their velocities with distance as far as $V < V_f$, though at much longer time scales. The crossover of $H(t)$ is depicted with a star in Figure 4.

3. Summary and Conclusions

In this paper, two additional aspects of UNIMOUN have been addressed, namely:

- UNIMOUN accommodates nicely the observational fact that the galaxies in the local universe recede at much slower rates than their distant counterparts?
- The Hubble parameter is a slowly varying function with the cosmic time: it starts with higher values in the early universe and decreases toward small ones in the far future, which is a causally consistent trend.

Based on the time-dependent $\mathcal{H}$-metric, both the analytical and GR-hydrodynamical calculations confirm that the newly created normal matter in the innermost region of the fireball was gravitationally bound. Once the matter has cooled down, the contraction would lead to the formation of galaxies that we observe today in the local universe. Nonetheless, the expansion of spacetime forces these galaxies to recede at relatively low rates, which is a consequence of the minimum energy theorem applied to a fireball with a finite mass.

Our study also confirms that the Hubble parameter is, in fact, a slowly varying function of cosmic time. Its value in the early times must have been higher than in the late universe, which is a self-consistent behaviour in UNIMOUN. Here the matter and momentum transferred from the fireball to G_B-type galaxies must have been sufficient to accelerate their motions up to relativistic velocities observed today as high redshift galaxies. The reason, therefore, is that although the spacetimes inside these galaxies are locally curved, the ambient parent spacetime is flat. Therefore, due to momentum conservation, any external bombardments of these levitating galaxies in the flat parent universe must set them into accelerating motions.

We note here that the "early universe" in ΛCDM-cosmologies differs fundamentally from that in UNIMOUN: While extremely high redshift galaxies in ΛCDM-cosmologies correspond to those that were formed shortly after the BB, in UNIMOUN, however, they may correspond to old and inactive galaxies that populated the ambient space of the BB, but started receding due to bombardment by the fireball to be seen today as very high redshift galaxies. In fact, the data from the CMB with/without Planck gives rise to a Hubble constant of roughly 67 $km \cdot s^{-1} \cdot Mpc^{-1}$, which is lower than the value revealed by Cepheids-SNIa measurements. This implies that H_0 would increase rather than decrease with cosmic time as predicated by UNIMOUN. Recalling the sensitivity of the CMB-Planck data to the underlying cosmological model, we conclude that UNIMOUN is a viable alternative to ΛCDM-cosmologies.

Acknowledgements

The author acknowledges the financial support of the IWR and KAUST. Max Camenzind, Mario Livio and Adi Nasser are acknowledged for their valuable comments and suggestions.

Conflicts of Interest

The author declares no conflicts of interest regarding the publication of this paper.

References

[1] Bahcall, N.A. (2015) *PNAS*, **112**, 3173-3175. https://doi.org/10.1073/pnas.1424299112

[2] Di Valentino, E., Mena, O., *et al.* (2021) *Classical and Quantum Gravity*, **38**, Article ID: 153001.

[3] Dianotti, M.G., De Simone, B., *et al.* (2021) *The Astrophysical Journal*, **912**, 150. https://doi.org/10.3847/1538-4357/abeb73

[4] Riess, A.G., *et al.* (2019) *The Astrophysical Journal*, **876**, 85. https://doi.org/10.3847/1538-4357/ab1422

[5] Aghanim, N., *et al.* (2020) *A&A*, **641**, A5-A6.

[6] Caroll, S.M. (2001) *LRR*, **4**, 1.

[7] Perlmutter, S. *et al.* (1999) *The Astrophysical Journal*, **517**, 565.

[8] Sato, K. (1981) *Monthly Notices of the Royal Astronomical Society*, **195**, 467-479. https://doi.org/10.1093/mnras/195.3.467

[9] Steinhardt, P.J. (2011) *Scientific American*, **304**, 18. https://doi.org/10.1038/scientificamerican0311-18b

[10] Hujeirat, A.A. (2021) *Journal of Modern Physics*, **12**, 7.

[11] Hujeirat, A.A. and Samtaney, R. (2019) *Journal of Modern Physics*, **10**, 1696-1712. https://doi.org/10.4236/jmp.2019.1014111

[12] Hujeirat, A. and Samtaney, R. (2020) *Journal of Modern Physics*, **11**, 1779-1784. https://doi.org/10.4236/jmp.2020.1111110

[13] Eskola, K.J. (2019) *Nature Physics*, **15**, 1111-1112. https://doi.org/10.1038/s41567-019-0643-0

[14] Espinoza, C.M., Lyne, A.G., Stappers, B.W. and Kramer, C. (2011) *Monthly Notices of the Royal Astronomical Society*, **414**, 1679-1704. https://doi.org/10.1111/j.1365-2966.2011.18503.x

[15] Roy, J., Yashwant Gupta, Y. and Lewandowski, W. (2012) *Monthly Notices of the Royal Astronomical Society*, **424**, 2213-2221. https://doi.org/10.1111/j.1365-2966.2012.21380.x

[16] Abbott, *et al.* (2017) *The Astrophysical Journal*, **848**, L12.

[17] Hujeirat, A.A. (2018) *Journal of Modern Physics*, **9**, 4.

[18] Camenzind, M. (2007) Compact Objects in Astrophysics. Springer, Heidelberg.

[19] Hujeirat, A.A. and Samtaney, R. (2020) *Journal of Modern Physics*, **11**, 395-406. https://doi.org/10.4236/jmp.2020.113025

[20] Hujeirat, A.A. (2022) *Journal of Modern Physics*, **13**, 1581-1597. https://doi.org/10.4236/jmp.2022.1312096

[21] Brousso, R. (2002) *Reviews of Modern Physics*, **74**, 825-874. https://doi.org/10.1103/RevModPhys.74.825

[22] Trimble, V. (1987) *Annual Review of Astronomy and Astrophysics*, **25**, 425-472. https://doi.org/10.1146/annurev.aa.25.090187.002233

[23] Hujeirat, A.A. (2022) *Journal of Modern Physics*, **13**, 1474-1498. https://doi.org/10.4236/jmp.2022.1311091

[24] Hujeirat, A.A. (2005) *Computer Physics Communications*, **168**, 1-24. https://doi.org/10.1016/j.cpc.2005.01.013

[25] Fischer, M.S. and Hujeirat, A.A. (2020) Time-Implicit Schemes in Fluid Dynamics?—Their Advantage in the Regime of Ultra-Relativistic Shock Fronts. https://ui.adsabs.harvard.edu/abs/2020arXiv200412310F/abstract

[26] Verlinde, E.P. (2010) *Journal of High Energy Physics*, **1104**, 29.